

# CONSTRUCTION OF DEFORMATION DIAGRAMS OF CONCRETE UNDER SHEAR BASED ON THE AUTHOR'S THEORY OF ANISOTROPIC MATERIALS POWER RESISTANCE TO COMPRESSION AND DEFORMATION THEORY OF PLASTICITY

*Boris S. Sokolov<sup>1</sup>, Oleg V. Radaikin<sup>2</sup>*

<sup>1</sup> JSC "Kazan GIPRONIIAVIAPROM", Kazan, RUSSIA

<sup>2</sup> Kazan State University of Architecture and Engineering, Kazan, RUSSIA

**Abstract:** The Aim of this work was the construction of a concrete deformation diagrams under shear on the basis of two approaches: the theory of anisotropic materials force resistance in compression and deformation theory of plasticity with the use of state diagrams of concrete under tension and compression, obtained by the authors jointly with Acad. N.I. Karpenko earlier. For this purpose, in the framework of the first approach, the main computational expression of the author's model was written in the current deformations, which ultimately allowed to establish a relationship between the diagrams  $\sigma_b-\varepsilon_b$ ,  $\sigma_{bt}-\varepsilon_{bt}$  and  $\tau_b-\gamma_b$  and reveal the mechanics of destruction of concrete elements under compression. The second approach additionally takes into account the change in the coefficient of transverse deformations,  $\mu_b$ , and shear modulus of deformations,  $G_b$ , as the load increases, but does not take into account the presence of normal stresses affecting the stress-strain state. This approach recreates the conditions of pure shear, which is possible only theoretically, and in real designs is applicable with a certain degree of error. Nevertheless, both approaches provide almost identical data in the construction of diagrams « $\tau_b-\gamma_b$ », which differ from the experiment by no more than 13-15%. In this regard, they are recommended for implementation: the first-to perform engineering calculations «manually», the second –to develop computer programs that allow you to automate the calculation.

**Keywords:** theory of anisotropic materials force resistance in compression, deformation theory of plasticity, diagram of concrete deformation at shear, shear strength

## К ПОСТРОЕНИЮ ДИАГРАММ ДЕФОРМИРОВАНИЯ БЕТОНА ПРИ СДВИГЕ НА ОСНОВЕ АВТОРСКОЙ ТЕОРИИ СИЛОВОГО СОПРОТИВЛЕНИЯ АНИЗОТРОПНЫХ МАТЕРИАЛОВ СЖАТИЮ И ДЕФОРМАЦИОННОЙ ТЕОРИИ ПЛАСТИЧНОСТИ

*Б.С. Соколов<sup>1</sup>, О.В. Радайкин<sup>2</sup>*

<sup>1</sup> АО «Казанский Гипронииавиапром», г. Казань, РОССИЯ

<sup>2</sup> Казанский государственный архитектурно-строительный университет, г. Казань, РОССИЯ

**Аннотация:** Целью данной работы ставилось построение диаграммы деформирования бетона при сдвиге на основе двух подходов: теории силового сопротивления анизотропных материалов сжатию и деформационной теории пластичности с использованием диаграмм состояния бетона при растяжении и сжатии, полученных авторами совместно с акад. Н.И. Карпенко ранее. Для этого в рамках первого подхода основное расчётное выражение авторской модели было записано в текущих деформациях, что в конечном итоге позволило установить взаимосвязь между диаграммами  $\sigma_b-\varepsilon_b$ ,  $\sigma_{bt}-\varepsilon_{bt}$  и  $\tau_b-\gamma_b$  и раскрыть механику разрушения бетонных элементов, находящихся в условиях сжатия. Во втором подходе дополнительно учитывает изменение коэффициента поперечных деформаций,  $\mu_b$ , и сдвигового модуля деформаций,  $G_b$ , по мере увеличения нагрузки, но не учтено наличие нормальных напряжений, влияющих на напряжённо-деформированное состояние. Этот подход воссоздаёт условия чистого сдвига,

что возможно лишь теоретически, а в реальных конструкциях применимо с определённой долей погрешности. Тем не менее оба подхода дают практически совпадающие данные при построении диаграмм « $\tau_b-\gamma_b$ », которые отличаются от эксперимента не более, чем на 13-15%. В связи с этим они рекомендованы для внедрения: первый – для выполнения инженерных расчётов «вручную», второй – для разработки компьютерных программ, позволяющих автоматизировать расчёт.

**Ключевые слова:** теория силового сопротивления анизотропных материалов сжатию, деформационная теория пластичности, диаграмма деформирования бетона при сдвиге, прочность на срез

The problem of reliable construction of diagrams of concrete deformation under shear arises when solving a number of practical and theoretical problems. For example, this concerns the calculations of reinforced concrete elements under bending in the zone of couple action of bending moments and shear forces, the adhesion of reinforcement to concrete, and the application of the theory of power resistance of anisotropic materials under compression to estimate the stress-strain state of structural elements at all stages of loading. This theory has been known for over 30 years, and in practice, it has shown its viability. Its main provisions at the present stage are set forth in the monograph [1]. However, the development potential of the theory is far from exhausted. Therefore, if the ultimate states of compressed concrete and reinforced concrete elements were examined at the stage of destruction in previous publications mainly, then this article attempts to study the intermediate stages of operation of these elements under load using diagrammatic calculation methods.

Below two approaches for constructing concrete shear deformation diagrams are given: 1 – The author's theory of the power resistance of anisotropic materials to compression [1]; 2 – Deformation theory of plasticity and design expressions for diagrams of concrete deforming under tension and compression, proposed in [2-4].

Figure 1 shows the design scheme for assessing the strength of a compressed element (prism and cylinder), reflecting the hypothesis of the author's theory [1] on the fracture mechanics that occurs after overcoming the material's resistance to separation, shear and crushing.

The strength condition according to the theory is written as the inequality:

$$N \leq N_{ult} = \frac{N_{bt} \cos \alpha + 2N_{sh}}{\sin \alpha} + N_{ef} \quad (1)$$

where  $N_{bt}, N_{sh}, N_{ef}$  are ultimate internal forces characterizing power resistance in the zones of stretching, shear and crushing;  $\alpha$  – wedge angle:

$$\alpha = \arctg(0,25 R_{bm} / R_{bm} - 1,56) \quad (2)$$

These efforts are determined as the product of the corresponding design resistance and area:

$$N_{bt} = R_{bt} A_{bt}, N_{sh} = R_{sh} A_{sh}, N_{ef} = R_b A_{ef}, \quad (3)$$

where  $R_{bt}, R_{sh}, R_b$  are respectively design resistance of concrete to tension, shear and compression, and  $A_{bt}, A_{sh}, A_{ef}$  are areas of tension, shear and crushing (compression). Substituting (2) in (1) and accepting

$$N = N_{ult} = R_b A,$$

where  $A$  is area of external effort transmitting, we obtain:

$$R_b A = R_{bt} A_{bt} \operatorname{ctg} \alpha + \frac{2R_{sh} A_{sh}}{\sin \alpha} + R_b A_{ef}. \quad (4)$$

At the same time formula (3) is the same for prismatic and cylindrical elements (fig. 1), but there is difference in determination of areas  $A_{bt}, A_{sh}, A_{ef}$  and substituting prismatic strength by cylindrical one  $f_{ck}$  (according to Eurocode-2), at the same time

$$f_{ck} \approx \frac{R_b}{\gamma_{ck} \gamma_R},$$

Construction of Deformation Diagrams of Concrete Under Shear Based on the Author's Theory of Anisotropic Materials Power Resistance to Compression and Deformation Theory of Plasticity

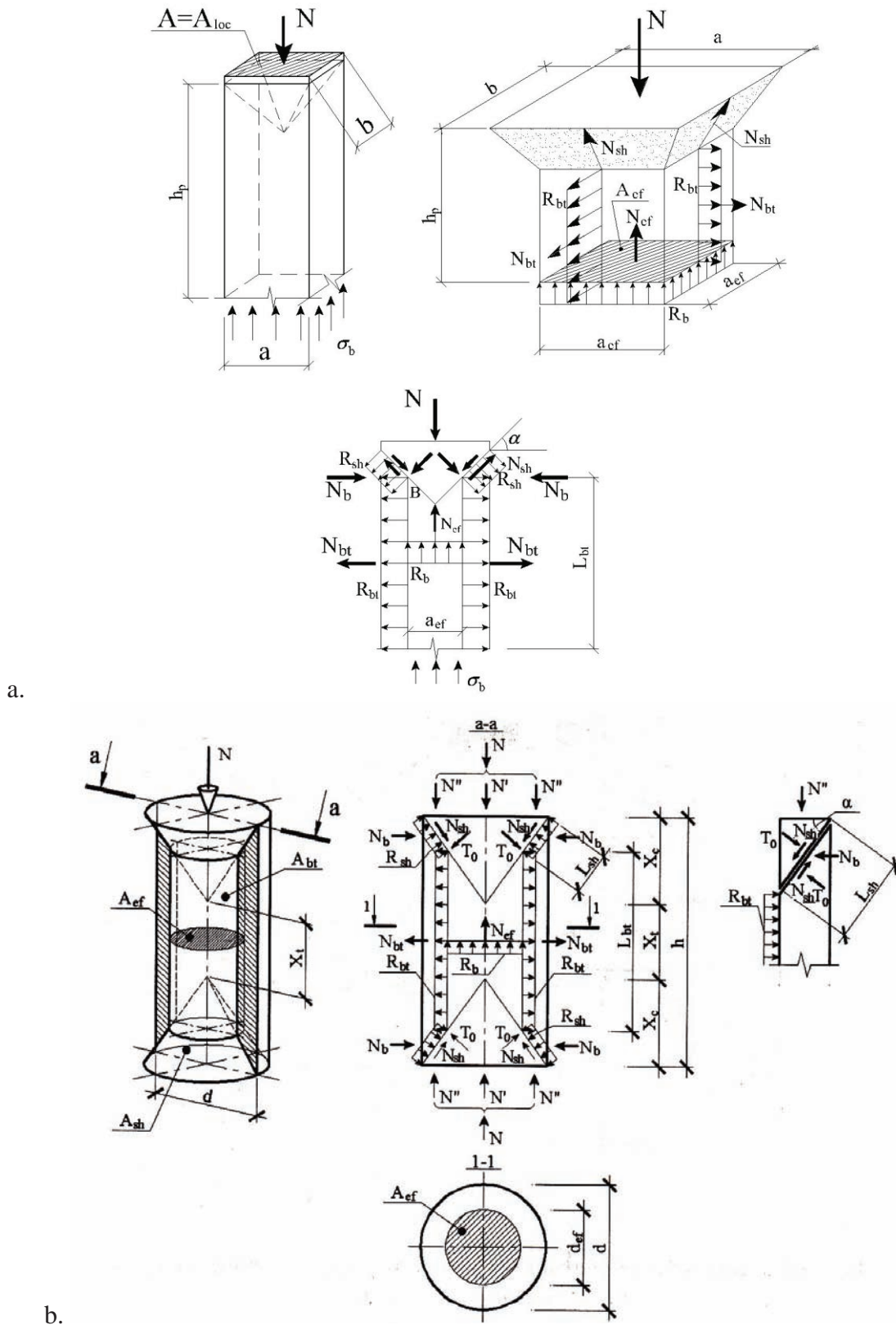


Figure 1. Calculation schemes of concrete prism (a) and cylinder (b) under compression.

where  $\gamma_{ck}=0,8$ ,  $\gamma_R=0,75$  are respectively coefficients of transition from cylindrical strength to cubic and from cubic to prismatic.

Let us transform expression (4) by following way:

$$R_b(A - A_{ef}) = R_{bt}A_{bt}ctg\alpha + \frac{2R_{sh}A_{sh}}{\sin\alpha} \Rightarrow R_b = k_1R_{bt}ctg\alpha + \frac{k_2R_{sh}}{\sin\alpha},$$

$$R_b(A - A_{ef}) = R_{bt}A_{bt}ctg\alpha + \frac{2R_{sh}A_{sh}}{\sin\alpha} \Rightarrow R_b = k_1R_{bt}ctg\alpha + \frac{k_2R_{sh}}{\sin\alpha}, \quad (5)$$

where  $k_1 = A_{bt}/(A - A_{ef})$ ,  $k_2 = 2A_{sh}/(A - A_{ef})$ .

Let us note that according to expression (5), it is possible to obtain the calculated value of concrete shear resistance depending on its class after the following transformation:

$$R_{sh} = \frac{R_b \sin\alpha - k_1R_{bt} \cos\alpha}{k_2}. \quad (6)$$

In addition, the same expression can be written through stresses, which will allow us to consider not only the stage of destruction of the concrete element, but also the intermediate stages of its loading:

$$\sigma_b = k_1\sigma_{bt}ctg\alpha + \frac{k_2\tau_b}{\sin\alpha}. \quad (7)$$

The resulting expression can now be written through the corresponding deformations:

$$\varepsilon_b E_b = k_1\varepsilon_{bt}E_{bt}ctg\alpha + \frac{k_2\gamma_b G_b}{\sin\alpha}. \quad (8)$$

According to Building standard of Russian Federation SP 63.13330.2012, it is:  $E_{bt} = E_b$ ,  $G_b = 0,4E_b$ , and at calculation by deformations, it is  $E_{bt} \approx 0,5E_b$ , then equality (8) can be written in the form:

$$\varepsilon_b = 0,5k_1\varepsilon_{bt}ctg\alpha + \frac{0,4k_2\gamma_b}{\sin\alpha}, \quad (9)$$

From equality (9), it follows: if we know the relative deformations of concrete under compression and tension, and their diagrams are given in the regulatory documents (Fig. 3, a-b), we can determine the relative deformations under shear:

$$\gamma_b = \frac{(\varepsilon_b - 0,5k_1\varepsilon_{bt}ctg\alpha)\sin\alpha}{0,4k_2}. \quad (10)$$

Substituting shear deformations in the expression

$$\tau_b = G_b\gamma_b \approx 0,4E_b\gamma_b,$$

we obtain diagram “ $\tau_b - \gamma_b$ ”. In this case, a significant difference in the values of ultimate deformation of concrete under compression and tension should be taken into account. The consequence of this is that when testing real samples (prisms or cylinders) for compression, vertical cracks appear, indicating the exhaustion of the tensile strength of concrete. In this case, in condition (10), from a certain level of loading, tensile deformations  $\varepsilon_{bt}$  should be excluded. Then the transverse expansion of the sample occurs due to the opening of vertical cracks, and at the moment immediately before the formation of these cracks, condition (10) will look like:

$$\gamma_{b1} = \frac{(\varepsilon_{b1} - 0,5k_1\varepsilon_{bt2}ctg\alpha)\sin\alpha}{0,4k_2}, \quad \tau_{b1} = 0,4E_b\gamma_{b1}, \quad (11)$$

where  $\varepsilon_{bt2}$  is ultimate deformation of concrete at tension ( $\varepsilon_{bt2} = 0,00015$ );

$$\varepsilon_{b1} = \frac{0,6R_b}{E_b}$$

is the boundary of elastic stage of compressed concrete work.

Value  $\gamma_{b1}$ , according to (11), is the abscissa of the first point from the parametric points in the

diagram “ $\tau_b - \gamma_b$ ”, which corresponds reaching value

$$\tau_b \approx 0,2R_{sh}$$

by tangential stresses.

The second parametric point is determined for conditions

$$\varepsilon_b = \varepsilon_{b0} = \frac{R_b}{E_b} \text{ and } \varepsilon_{bt} = 0$$

that means concrete in tension excluded from work, and transverse expansion of a sample occurs due to opening of vertical cracks. At the same time, tangential stresses reaches maximum values:

$$\gamma_{b0} = \frac{\varepsilon_{b0} \sin \alpha}{0,4k_2}, \tau_{b0} = R_{sh}. \quad (12)$$

The third parametric point corresponds to the ultimate strain of compressed concrete

$$\varepsilon_b = \varepsilon_{b2} = 0,002$$

and, by analogy with the previous one, we obtain:

$$\gamma_{b2} \approx \frac{\varepsilon_{b2} \sin \alpha}{0,4k_2}, \tau_{b2} = \tau_{b0} = R_{sh}. \quad (13)$$

With a further increase in load, we assume that the concrete shear resistance is overcome and

the compressed core continues to work. However, the friction and engagement forces arising between concrete surfaces along inclined platforms should also provide some resistance up to the complete destruction of the compressed element.

The verification of the calculated expressions was carried out according to the results of concrete samples of a cylindrical shape [1]. The nature of the formation and development of cracks for specimens of the 5.1 series ( $d \times h = 0.1 \times 0.2$  m, concrete B30) is shown in Fig. 2, from which one can see their compliance with the design scheme and the hypothesis of the fracture mechanism.

For the specimens of the considering series, the results of calculating the parameters included in formula (6), as well as their breaking load, are given in the table below, which also shows a comparison of theoretical and experimental data. From table, it is seen:

$$R_{sh}/R_{bt} = 2,944$$

that proves known relationship

$$R_{sh}/R_{bt} = \sqrt{R_b/R_{bt}} \approx 3,0$$

[5]. Besides, difference between theoretical and experimental values of ultimate force  $N_{ult}$  is 13.5 % that can be accepted as satisfactory result for such a material with high variability of properties as concrete.

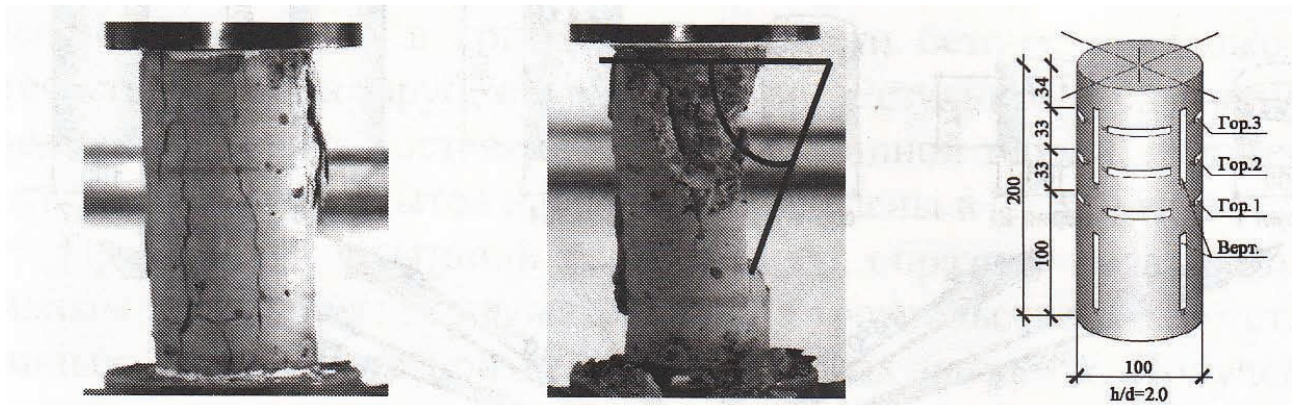


Figure 2. The nature of the destruction of cylindrical specimens under compression [1].

Table 1. Comparison of theoretical and experimental data for specimens series of 5.1 [1].

Parameter	$R_b$ , MPa	$R_{bt}$ , MPa	$\alpha$ , °	$k_1$	$k_2$	$R_{sh}$ , MPa	$N_{ult}$ , ton
Theory	-	-	54 <sup>0</sup>	10,14	3,43	5,01	21,0
Experiment	20,1	1,7	57 <sup>0</sup>	-	-	-	18,5

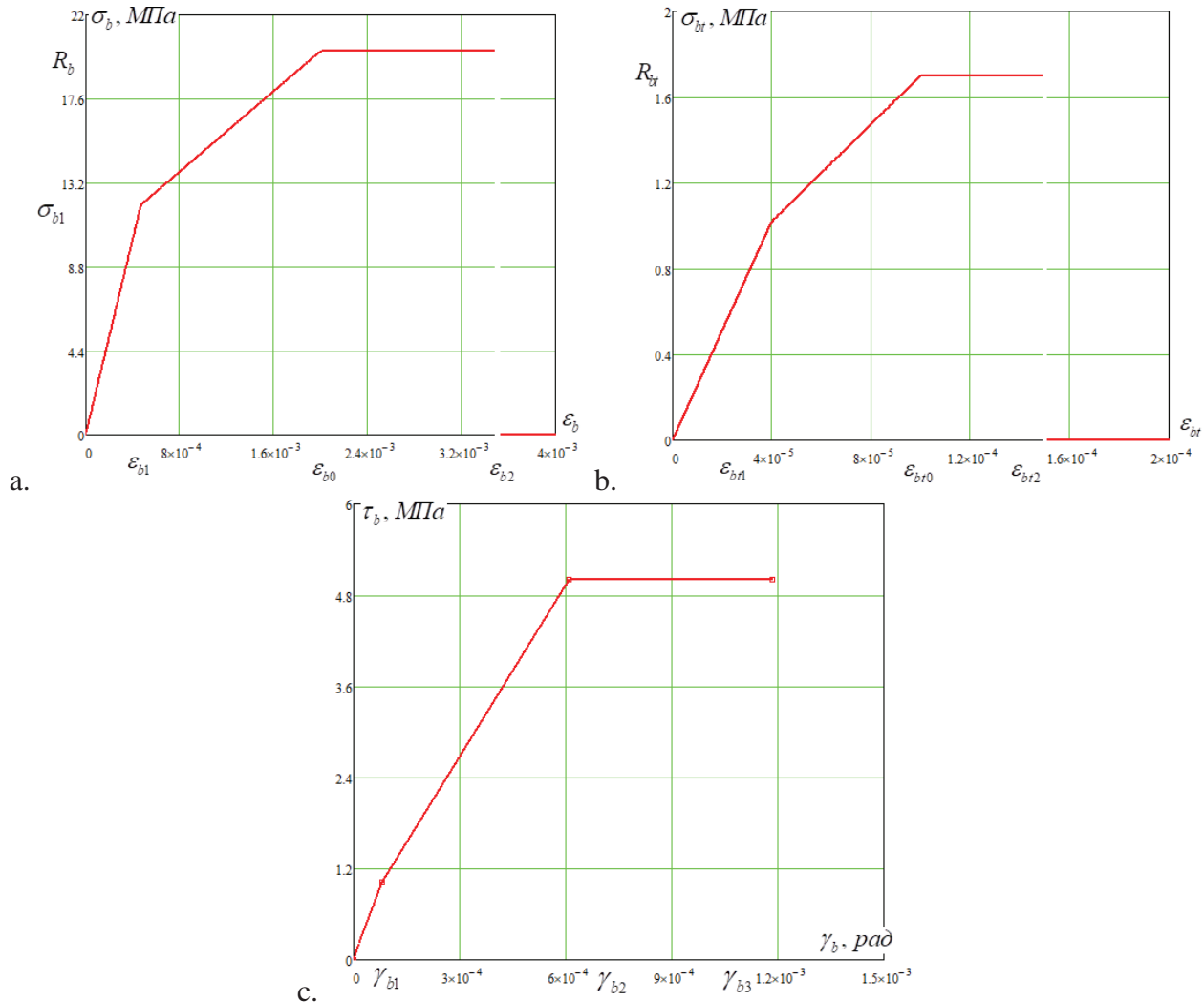


Figure 3. Concrete deformation diagrams for a cylindrical specimen of the 5.1 series [1] made of class B30 concrete under compression (a), tension (b) and shear (c).

In addition, fig. 3, a-b show the so-called working (three-line) diagrams of concrete deforming under compression and tension, which are constructed according to the formulas of SP 63.13330.2012. Figure 3,c shows the diagram “ $\tau_b - \gamma_b$ ” obtained from dependencies (11)-(13).

To identify the relationship between the diagrams of deformation of concrete under compression, tension and shear with each other,

we superimposed all three graphs in Figure 3 to one coordinate plane. In order to do this, for each diagram we took our scale of the stress axis, and we expressed the tensile and shear strains through compression strains:

$$\epsilon_{bt} = \mu \epsilon_b \approx 0,2 \epsilon_b, \gamma_b = \frac{\epsilon_b \sin \alpha}{0,4 k_2}.$$

Then we obtain diagram presented in Figure 4.

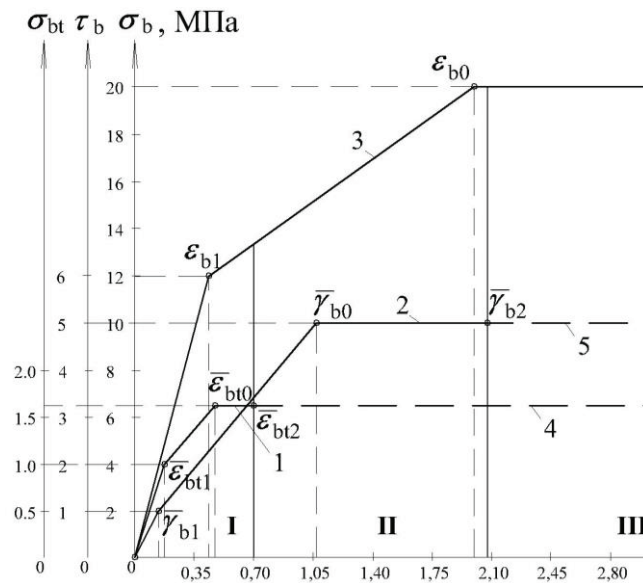


**Figure 4.** Diagrams of deformation of a cylindrical specimen of a series 5.1 [1] of concrete of class B30 under tension - 1, shear - 2 and compression - 3; 4 - section of the disclosure of vertical cracks; 5 - plot of resistance due to friction and engagement of concrete surfaces; I, II, III - areas of the characteristic operation of the element at different stages of loading.

In this figure, for diagrams 1 and 2, parametric points are indicated by deformations, which are determined using the above dependencies:

$$\bar{\varepsilon}_{bt} = \frac{\varepsilon_{bt}}{0,2}, \quad \bar{\gamma}_b = \frac{0,4k_2}{\sin \alpha} \gamma_b.$$

At the same time, three characteristic areas can be distinguished in compression diagram 3: I – the area of joint resistance to compression of the separation, shear and crushing zones; II – the area of switching off the separation zone from work and further joint resistance to compression of the shear and crushing zones; III - the area of switching off the shear zone from work and further resistance to compression of only the crushing zone.

Figure 4 also shows that the abscissas of the majority of the parametric points of the three strain diagrams practically coincide (excluding  $\bar{\gamma}_{b0}$ ):

- $\bar{\varepsilon}_{bt1} = \bar{\gamma}_{b1}$  is the condition of the beginning of inelastic deformations in the separation zone;
- $\bar{\varepsilon}_{bt0} = \varepsilon_{b1}$  is condition of nucleation of vertical cracks of transverse separation, their

development, continuing up to deformations  $\bar{\varepsilon}_{bt2}$ , after that stretched zone removing from work (boundary between areas I and II);

- $\bar{\gamma}_{b2} = \varepsilon_{b0}$  – after the shear zones are completely turned off, crushing of the concrete core begins (the boundary between regions II and III).

Moreover, after the magnitude reached in the stretched zone of deformations  $\varepsilon_{bt} = \varepsilon_{bt2}$ , the tensile diagram 1 continues in the form of a dashed section 4, which characterizes the opening of vertical cracks. In addition, for the shear diagram 2 after reaching the deformations  $\gamma_b = \gamma_{b2}$ , the dashed section 5 characterizes the work of the friction forces and the engagement of concrete surfaces on inclined platforms.

Thus, using the author's theory, we obtained analytical expressions for determining concrete deformations under shear and tangential stresses during fracture of the material, which allowed us to finally represent the dependence “ $\tau_b - \gamma_b$ ” (Figure 3, c). In addition, the mechanics of concrete deformation under compression up to its destruction were explained on the basis of this theory, which became possible due to the establishment of the relationship of concrete

deformation diagrams for tension, compression and shear.

The second approach to constructing the “ $\tau_b - \gamma_b$ ” dependence is using the provisions of the deformation theory of plasticity [6] and the diagrams proposed by Acad. Karpenko N.I. together with the authors of this article [2-4].

This theory is based on the results of testing concrete prisms for compression with the determination of longitudinal and transverse strains ( $\varepsilon_b$  and  $\varepsilon'_b$ ). Using well-known expressions [6], the desired parameters for describing the diagrams can be obtained by the following algorithm:

Initial experimental data:  $\sigma_b = f(\varepsilon_b)$ ,  $\mu_b = \frac{\varepsilon'_b}{\varepsilon_b}$ ;

(14)

Solution algorithm:  $\gamma_b = (1 + \mu_b)\varepsilon'_b \rightarrow E'_b = \frac{\sigma_b}{\varepsilon_b} \rightarrow G'_b = \frac{E'_b}{2(1 + \mu_b)} \rightarrow \tau_b = G'_b \gamma_b$ ,

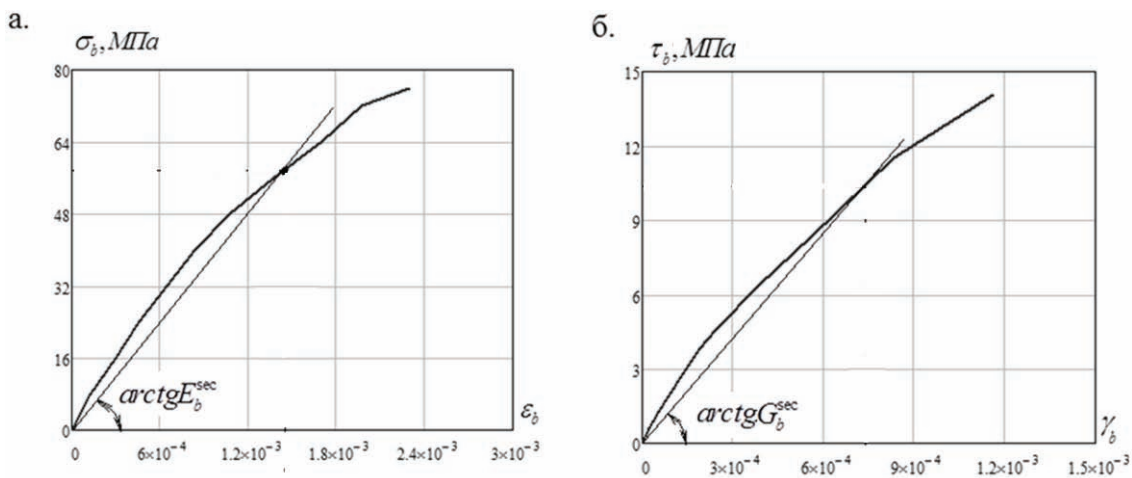


Figure 4. Deformation diagrams for high-strength concrete of class B100: a – experimental “ $\sigma_b - \varepsilon_b$ ” [8]; b – “ $\tau_b - \gamma_b$ ”, constructed on the basis of algorithm (14).

where  $\mu_b$  is coefficient of transverse deformations, which increases from initial value  $\mu_b^0 = 0,15 \dots 0,2$  up to 0.5.

Figure 4b shows a curve constructed according to the proposed algorithm (14) based on experimental data [8] for high-strength concrete of class B100.

When there are not experimental data, this coefficient can be obtained analytically by the formula proposed Acad. N.I. Karpenko [7]:

$$\mu_b = \bar{\mu}_b \pm (\mu_b^0 - \bar{\mu}_b) \sqrt{1 - \eta^2}, \quad (15)$$

where

$$\bar{\mu}_b = \mu_b^0 + 1 - \sqrt[3]{\frac{R_{bn}}{\varepsilon_{b0} E_b}}$$

is the lateral strain coefficient at the top of the compression diagram;

$$\varepsilon_{b0} \approx 0,002$$

is the relative compressive strains at the same point;

$$\mu_b^0 = 0,2$$

is Poisson coefficient;

$$\eta = \frac{\sigma_b}{R_{bn}}$$

is current level of stresses.

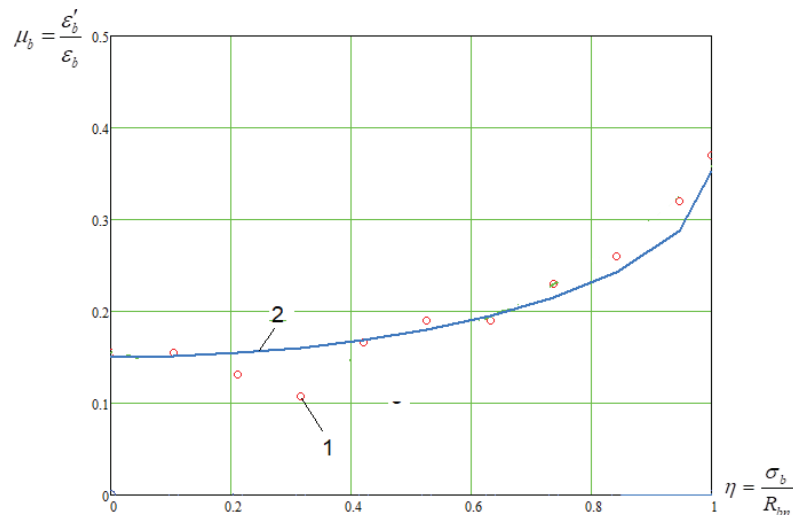


Figure 5. Change in the coefficient of transverse deformations "μ<sub>b</sub>" during loading a compressed prism of concrete class B100: 1 – experimental data [8]; 2 – curve constructed by the formula (15).

For concrete of class B100, the experimental and theoretical dependences for μ<sub>b</sub> are shown in Figure 5.

The curves obtained in this figure qualitatively and to some extent quantitatively coincide with the previously obtained data in the works of O.

J. Berg [9,10], which have already become classics and confirms the validity of the proposed expressions.

In the case of applying the analytical dependence for μ<sub>b</sub>, the algorithm (14) is slightly modified:

Initial analytical data:  $\sigma_b = f(\varepsilon_b)$  [2-4],  $\mu_b = \varphi(\eta)$ ;

$$\text{Solution algorithm: } \mu_b = \varphi \left[ \frac{f(\varepsilon_b)}{R_{bn}} \right] = \psi(\varepsilon_b) \rightarrow \gamma_b = (1 + \mu_b) \mu_b \varepsilon_b \rightarrow E'_b = \frac{\sigma_b}{\varepsilon_b} \rightarrow \quad (16)$$

$$G'_b = \frac{E'_b}{2(1 + \mu_b)} \rightarrow \tau_b = G'_b \gamma_b$$

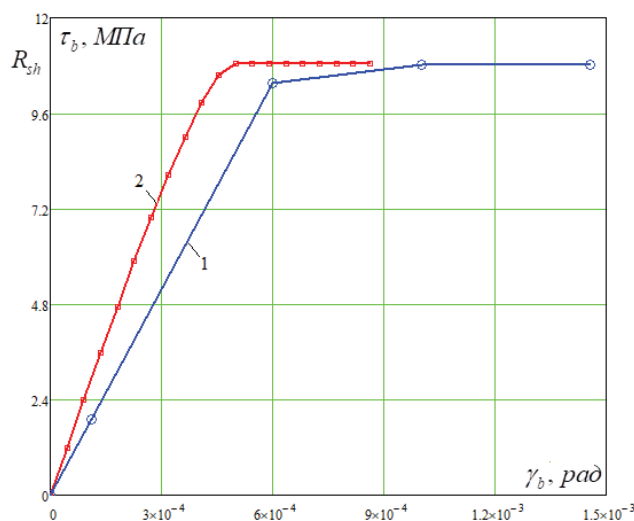


Figure 6. The diagram "τ<sub>b</sub>-γ<sub>b</sub>" for heavy concrete of class B100, constructed according to formulas (8)-(11) – curve 1 - and on the basis of the algorithm (16) – curve 2.

As a result of the implementation of this algorithm for concrete of class B100, we obtain the dependence “ $\tau_b-\gamma_b$ ”, presented in Figure 6 (curve 2). At the same time, for comparison, curve 1 is shown in the same figure, constructed according to formulas (8)-(11) of the previously considered approach.

Unlike Figure 4b, the curves in Figure 6 were built according to the normative strength characteristics of concrete. Nevertheless, the difference between the experimental and theoretical shear strength turned out to be

$$R_{sh}^{ex}/R_{sh}^{th}=14/11=1,27,$$

which approximately corresponds to the material safety factor  $\gamma_m=1,3$ . And despite the fact that, in contrast to the experimental curve, the diagrams in Figure 6 have a horizontal section (theoretically possible), however, in general, the values of the parametric points of the compared curves practically coincide.

Thus, the second approach to the construction of shear strain diagrams is considered. This approach is based on the provisions of the deformation theory of plasticity and the dependences of [2-4, 7]. It takes into account the change in the transverse strain coefficient,  $\mu_b$ , and the shear strain modulus,  $G'_b$ , as the load increases. However, the presence of normal stresses affecting the stress-strain state is not taken into account.

## CONCLUSIONS

- Two approaches to determining the diagrams of concrete deformation under shear are considered:
  - the author's theory of the power resistance of anisotropic materials to compression;
  - the deformation theory of plasticity and the provisions of [2-4, 7] developed by academician N.I. Karpenko together with the authors of this article.
- The peculiarity of the first approach is that it takes into account the specifics of concrete work

under compression, reveals the mechanics of its destruction from overcoming the peel, shear and crush resistance and is based on piecewise-linear diagrams of material deformation under compression and tension.

3. The second approach is based on the provisions of the deformation theory of plasticity and dependences for diagrams [2-4, 7], in addition, it takes into account the change in the coefficient of transverse deformations,  $\mu_b$ , and the shear modulus of deformations,  $G'_b$ , as the load increases. However, the presence of normal stresses affecting the stress-strain state is not taken into account, since the pure shear conditions are recreated in the calculation model of this approach, which is possible only theoretically, and in real designs it is applicable with a certain degree of error.

4. Comparing the mathematical apparatus of both approaches, we can conclude that the first one is more applicable for performing engineering calculations “manually”, while the second one can be recommended for the development of computer programs that automate the calculation (including programs based on the Finite Element Method). Nevertheless, both approaches give practically the same data when constructing the “ $\tau_b-\gamma_b$ ” diagrams, which differ from the experiment by no more than 13-15%. Therefore, the proposed approaches are recommended for implementation in the regulatory literature on the design of concrete and reinforced concrete elements and structures.

## REFERENCES

- Sokolov B.S.** Teoriya silovogo soprotivleniya anizotropnykh materialov szhatiyu i yeyo prakticheskoye primeneniye [The theory of force resistance of anisotropic materials to compression and its practical application]. Moscow, Izd-vo ASV, 2011, 160 pages (in Russian).
- Karpenko N.I., Sokolov B.S., Radaikin O.V.** Analiz i sovershenstvovaniye

- krivolineynykh diagramm deformirovaniya betona dlya rascheta zhelezobetonnykh konstruktsiy po deformatsionnoy modeli [Analysis and improvement of curved concrete deformation diagrams for calculating reinforced concrete structures using the deformation model]. // *Promyshlennoye i grazhdanskoye stroitel'stvo*, 2013, No. 1, pp. 25-27 (in Russian).
3. **Karpenko N.I., Sokolov B.S., Radaykin O.V.** Sovershenstvovaniye metodiki rascheta izgibayemykh zhelezobetonnykh elementov bez predvaritel'nogo napryazheniya po obrazovaniyu normal'nykh treshchin [Improving the methodology for calculating bent reinforced concrete elements without prestressing the formation of normal cracks]. // *Zhurnal Stroitel'nyye materialy*, 2013, No. 6, pp. 54-55 (in Russian).
  4. **Karpenko N.I., Sokolov B.S., Radaykin O.V.** K raschotu prochnosti, zhostkosti i treshchinostoykosti vnetsentrenno szhatykh zhelezobetonnykh elementov s primeneniym nelineynoy deformatsionnoy modeli [To the calculation of strength, rigidity and crack resistance of eccentrically compressed reinforced concrete elements using a nonlinear deformation model]. // *Izvestiya KazGASU*, 2013, No. 4 (26), pp. 113-120 (in Russian).
  5. **Bazhenov YU.M., Korol' Ye.A., Yerofeyev V.T., Mitina Ye.A.** Ograzhdayushchiye konstruktsii s ispol'zovaniym betonov nizkoy teploprovodnosti [Building envelopes using concretes of low thermal conductivity]. Moscow, Izd-vo ASV, 2008, 320 pages (in Russian).
  6. **Teregulov I.G.** Soprotivleniye materialov i Osnovy teorii uprugosti i plastichnosti. Uchebnik dlya studentov vuzov [Resistance of materials and Fundamentals of the theory of elasticity and plasticity. Textbook for university students]. Moscow, Vysshaya shkola, 1984, 472 pages (in Russian).
  7. **Karpenko N.I.** Obshchiye modeli mekhaniki zhelezobetona [General models of reinforced concrete mechanics]. Moscow, Stroyizdat, 1996, 416 pages (in Russian).
  8. **Punagin V.V.** Svoystva i tekhnologiya betona dlya vysotnogo monolitnogo stroitel'stva [Properties and technology of concrete for high-rise monolithic construction]. // *Elektronnyy arkhiv Khar'kovskogo natsional'nogo universiteta imeni V.N. Karazina* [Electronic archive of V.N. Karazin Kharkiv National University]. Khar'kov, 2012. URL: <http://dspace.snu.edu.ua:8080/jspui/bitstream/123456789/357/32/Punagin.pdf> (available on 12.05.2014). (in Russian).
  9. **Berg O.J., Shcherbakov Ye.N., Pisanko G.N.** Vysokoprochnyy beton [High strength concrete]. Moscow, Stroyizdat, 1971, 208 pages (in Russian).
  10. **Berg O.J.** Fizicheskiye Osnovy teorii prochnosti betona i zhelezobetona [Physical Fundamentals of the theory of strength of concrete and reinforced concrete]. Moscow, Gosstroyizdat, 1962, 98 pages (in Russian).

## СПИСОК ЛИТЕРАТУРЫ

1. **Соколов Б.С.** Теория силового сопротивления анизотропных материалов сжатию и её практическое применение. – М.: Издательство АСВ, 2011. – 160 с.
2. **Карпенко Н.И., Соколов Б.С., Радайкин О.В.** Анализ и совершенствование криволинейных диаграмм деформирования бетона для расчета железобетонных конструкций по деформационной модели. // *Промышленное и гражданское строительство*, 2013, №1, с. 25-27.
3. **Карпенко Н.И., Соколов Б.С., Радайкин О.В.** Совершенствование методики расчета изгибаемых железобетонных элементов без

предварительного напряжения по образованию нормальных трещин. // *Журнал Строительные материалы*, 2013, №6, с. 54-55.

4. **Карпенко Н.И., Соколов Б.С., Радайкин О.В.** К расчёту прочности, жёсткости и трещиностойкости внецентренно сжатых железобетонных элементов с применением нелинейной деформационной модели. // *Известия КазГАСУ*, 2013, №4 (26), с. 113-120.
5. **Баженов Ю.М., Король Е.А., Ерофеев В.Т., Митина Е.А.** Ограждающие конструкции с использованием бетонов низкой теплопроводности. – М.: Издательство АСВ, 2008. – 320 с.
6. **Терегулов И.Г.** Сопротивление материалов и Основы теории упругости и пластичности. – М.: Высшая школа, 1984. – 472 с.
7. **Карпенко Н.И.** Общие модели механики железобетона. – М.: Стройиздат, 1996. – 416 с.
8. **Пунагин В.В.** Свойства и технология бетона для высотного монолитного строительства. // *Электронный архив Харьковского национального университета имени В.Н. Каразина*. – Харьков, 2012. URL: <http://dspace.snu.edu.ua:8080/jspui/bitstream/123456789/357/32/Punagin.pdf> (дата обращения: 12.05.2014).
9. **Берг О.Я., Щербаков Е.Н., Писанко Г.Н.** Высокопрочный бетон. – М.: Стройиздат, 1971. – 208 с.
10. **Берг О.Я.** Физические Основы теории прочности бетона и железобетона. – М.: Госстройиздат, 1962. – 98 с.

Zhbikk, Kazan state University of Architecture and Construction; 420043, Russia, Republic of Tatarstan, Kazan, Zelenaya str., 1; e-mail: olegxxii@mail.ru.

Соколов Борис Сергеевич, член-корреспондент Российской академии архитектуры и строительных наук, профессор, доктор технических наук; научный консультант Акционерного общества «Казанский Гипронииавиапром»; 420127, Россия, Республика Татарстан, г. Казань, ул. Дементьева, 1; E-mail: sbs.1942@mail.ru.

Радайкин Олег Валерьевич, кандидат технических наук, доцент кафедры ЖБиКК Казанского государственного архитектурно-строительного университета; 420043, Россия, Республика Татарстан, г. Казань, ул. Зеленая, 1; e-mail: olegxxii@mail.ru.

---

Sokolov Boris Sergeevich, Correspondent Member of the Russian Academy of Architecture and Construction Sciences, Professor, Doctor of technical Sciences; scientific adviser, JSC “Kazan Giproniiaviaprom”; 420127, Russia, Republic of Tatarstan, Kazan, Dementyev St., 1; e-mail: sbs.1942@mail.ru.

Radaikin Oleg Valerjevich, Candidate of Technical Sciences, Associate Professor of the Department of